Bis 2,6-difluorophenoxide Dimeric Complexes of Zinc and Cadmium and Their Phosphine Adducts: Lessons Learned Relative to Carbon Dioxide/Cyclohexene Oxide Alternating Copolymerization Processes Catalyzed by Zinc Phenoxides

Donald J. Darensbourg,* Jacob R. Wildeson, Jason C. Yarbrough, and Joseph H. Reibenspies

Contribution from the Department of Chemistry, Texas A&M University, P.O. Box 30012, College Station, Texas 77842

Received August 2, 2000

Abstract: Dimeric phenoxide derivatives of zinc and cadmium have been synthesized from the reaction of the corresponding metal bistrimethylsilylamide and two equivalents of 2,6-$F_2C_6H_3OH$ in tetrahydrofuran. The zinc analogue, [Zn(O-2,6-$F_2C_6H_3)_2$·THF]$_2$ (**1**), has been characterized in the solid state via X-ray crystallography, where the zinc centers are shown to possess distorted tetrahedral geometry containing two bridging phenoxides and a terminal phenoxide and THF ligand. The distance between the metal centers (Zn···Zn) was found to be 3.059 Å, and the THF ligands lie on opposite sides of the plane formed by the two zinc atoms and two bridging phenoxide ligands' oxygen atoms. There are several Zn···F nonbonding distances involving the bridging phenoxide ligands that are less than the van der Waals internuclear distance. In addition, both the zinc and cadmium dimeric derivatives have been prepared such that the labile THF ligands are replaced by the sterically encumbering basic phosphine, PCy_3. The solid-state structures of [Zn(O-2,6-$F_2C_6H_3)_2$·PCy_3]$_2$ (**2**) and [Cd(O-2,6-$F_2C_6H_3)_2$·PCy_3]$_2$ (**5**) are similar to that of complex **1**, where the tricyclohexylphosphine ligands, like the THF ligands, are accommodated in a trans configuration. The ^{31}P NMR spectrum of complex **2** in C_6D_6 upon addition of free PCy_3 exhibits sharp resonances assigned to both the complex (9.58 ppm) and free PCy_3 (10.6 ppm), which is indicative of slow exchange of the phosphine ligands. On the other hand, the phosphine ligands on the cadmium derivative (**5**) are involved in an exchange process with free PCy_3 via a rapid equilibrium between **5** and two equivalents of Cd(O-2,6-$F_2C_6H_3)_2(PCy_3)_2$. The equilibrium reaction strongly favors the monomer cadmium bisphosphine complex at low temperature (−80 °C). As expected, the ^{113}Cd and ^{31}P NMR spectra of complex **5** in solution in the absence of excess PCy_3 is quite similar to that determined in the solid state by CP/MAS. Complex **1** and its chloro- and bromophenoxide analogues were shown to be effective catalysts for the copolymerization of cyclohexene oxide and CO_2, the terpolymerization of cyclohexene oxide/propylene oxide/CO_2, and the homopolymerization of cyclohexene oxide. In the case of the copolymerization process (80 °C and 55 bar), the polycarbonate copolymer that was produced is completely alternating, with no polyether linkages. At the same time, the homopolymerization of cyclohexene oxide to afford polyether in the presence of **1** as catalyst is much more facile than the copolymerization process. Importantly, for both copolymerization and homopolymerization processes catalyzed by complex **1**, the initiator of the polymer chain growth is a difluorophenoxide unit, as revealed by ^{19}F NMR, with both CO_2 insertion and epoxide ring-opening being involved in the initiation step. At 80 °C and 55 bar, the coupling of propylene oxide and CO_2 led almost exclusively to propylene carbonate. On the other hand, at lower temperatures (i.e., 40 °C), copolymer formation was favored over cyclic carbonate production. Because of the relative rates of copolymerization of cyclohexene oxide and carbon dioxide as a function of the halogen atom in the [Zn(O-2,6-$X_2C_6H_3)_2$·THF]$_2$ catalysts, that is, F > Cl > Br, activation of epoxide by the zinc center is proposed to be rate-limiting relative to the CO_2 insertion process.

Introduction

Utilizing the sterically encumbered aryloxide ligand containing *tert*-butyl substituents in the 2,6-positions of the aryl ring, Caulton and co-workers prepared the first well-characterized, soluble zinc aryloxide complexes.[1] That is, (2,6-di-*tert*-butylphenoxide)$_2$Zn(THF)$_2$ was obtained upon reacting Zn[N(SiMe$_3$)$_2$]$_2$ with 2,6-di-*tert*-butylphenol in tetrahydrofuran, and its structure was defined crystallographically. Prior to their report, the known zinc bis(alkoxides) or bis(aryloxides) were insoluble in common organic solvents and, hence, were presumed to be polymeric in structure.[2] Recently, we carried out rather comprehensive studies of the synthesis and structural characterization of soluble bisaryloxides of zinc[3,4] and their

(1) Geerts, R. L.; Huffman, J. C.; Caulton, K. G. *Inorg. Chem.* **1986**, *25*, 1803.

(2) Mehrotra, R. C. *Adv. Inorg. Chem. Radiochem.* **1983**, *26*, 269.

(3) Darensbourg, D. J.; Holtcamp, M. W. *Macromolecules* **1995**, *28*, 7577.

(4) Darensbourg, D. J.; Holtcamp, M. W.; Struck, G. E.; Zimmer, M. S.; Niezgoda, S. A.; Rainey, P.; Robertson, J. B.; Draper, J. D.; Reibenspies, J. H. *J. Am. Chem. Soc.* **1999**, *121*, 107.

10.1021/ja002855h CCC: $19.00
Published on Web 12/02/2000

phosphine adducts.[5] These investigations were stimulated by the potential use of these derivatives as catalysts for the coupling reaction of carbon dioxide and epoxides to afford polycarbonates and/or cyclic carbonates. Indeed, these complexes represent the first reported catalysts for the coupling of CO_2 and cyclohexene oxide to provide high-molecular-weight polycarbonates which exhibited greatly enhanced reactivity over earlier published work.[6] Since these studies, several other active zinc catalysts for these processes have been discovered.[7−10]

By way of contrast, when the bis-(2,6-di-*tert*-butylphenolate)-zinc complex is isolated from a hydrocarbon solvent, it crystallizes as a dimeric species containing two trigonal zinc metal centers, each with two bridging and one terminal aryloxides.[1,11] This structure is similar to those we reported for the monomeric, anionic derivatives of zinc and cadmium, for example, $[K(THF)_6][Zn(O\text{-}2,6\text{-}t\text{-}Bu_2C_6H_3)_3]$. In this latter instance, there are no bound THF molecules, even though several are contained in the crystal lattice. Evidently, the arrangement of three bulky phenoxides will not allow for the additional binding of bases. Consistent with this conclusion is the observation that this latter zinc derivative is ineffective at binding(activating) epoxides for CO_2 coupling reactions.

In continuation of our previous work on bis-phenoxides of zinc and their role as catalysts for coupling reactions of carbon dioxide and epoxides, we report here on several zinc complexes that were derived from phenols that were substituted in the 2,6-positions with sterically less-crowded, electron-withdrawing halogen groups. In these instances, we have generated dimeric species from THF solution which have been shown by X-ray crystallography to contain tetrahedrally coordinated zinc centers. That is, in addition to the two bridging and one terminal phenolate ligands, there is a THF molecule bound to each zinc. These zinc derivatives represent the most effective phenoxide catalysts for producing polycarbonates from CO_2/epoxides that we have thusfar uncovered. Furthermore, unlike the other reported complexes, these remain stable and maintain their catalytic activity when stored in moist air. Although the increase in catalytic effectiveness of these phenolates of zinc is not of major significance, there are several important lessons to be learned with regard to the mechanistic aspects of this process from their use. These include questions of initiator(polymer end group) and polyether formation. We have described here, as well, complimentary investigations of the cadmium analogues. Incorporated into these latter studies are solution and solid-state ^{113}Cd NMR measurements which compare the structures of these complexes in both states to each other as well as to the corresponding zinc derivatives.

Experimental Section

Methods and Materials. Unless otherwise specified, all syntheses and manipulations were carried out on a double-manifold Schlenk vacuum line under an atmosphere of argon or in an argon-filled glovebox. Glassware was flamed out thoroughly prior to use. Solvents were freshly distilled from sodium benzophenone before use. Cyclohexene oxide and propylene oxide were purchased from Aldrich Chemical Co. and purified by distillation over calcium hydride. Bone dry carbon dioxide was purchased from Scott Specialty Gases, Inc. 2,6-difluorophenol, 2,6-dichlorophenol, 2,6-dibromo-4-methylphenol, and tricyclohexylphosphine were purchased from Aldrich Chemical Co. and were sublimed and stored in a glovebox prior to use. $Zn[N(SiMe_3)_2]_2$ and $Cd[N(SiMe_3)_2]_2$ were prepared according to published literature,[13] stored in the glovebox, and used immediately after removal from the box. K(2,6-difluorophenoxide) was synthesized and isolated from the reaction of KH with the corresponding phenol in THF. Infrared spectra were recorded on a Mattson 6081 spectrometer with DTGS and mercury cadmium telluride (MCT) detectors. All isotopically labeled solvents for NMR experiments were purchased from Cambridge Isotope Laboratories. ^1H and ^{13}C NMR spectra were recorded on Varian XL-200E, Unity +300 MHz, and VXR 300 MHz superconducting high-resolution spectrometers. ^{19}F and ^{31}P data were acquired on a Unity +300 MHz superconducting NMR spectrometer operating at 282 and 121 MHz, respectively. All ^{19}F NMR data are referenced to 10% $CFCl_3$ and 1% $CClH_2CClF_2$ in acetone-d_6, whereas all ^{31}P NMR data are referenced to H_3PO_4 (85% in D_2O). Solution-state ^{113}Cd spectra were recorded on a Varian XL-400E superconducting high-resolution spectrometer operating at 88 MHz and using an external 0.1 M $Cd(ClO_4)_2/D_2O$ reference. Solid-state ^{113}Cd spectra were recorded on a Bruker MSL 300 superconducting spectrometer using an external $Cd(ClO_4)_2$ reference and operating at 66.546 MHz. Elemental analyses were carried out by Galbraith Laboratories, Inc.

Note! Cadmium compounds and their wastes are extremely toxic and must be handled carefully. Cadmium waste products should be stored in a separate clearly-marked container.

Synthesis of $[(2,6\text{-Difluorophenoxide})_2Zn]_2(THF)_2$, (1). A 5-mL THF solution of 2,6-difluorophenol (0.135 g, 1.04 mmol) was added to a 5-mL THF solution of $Zn[N(SiMe_3)_2]_2$ (0.20 g, 0.52 mmol), resulting in a clear colorless solution which was stirred at room temperature for 2 h. The solution was then concentrated to 5 mL and placed in a freezer at −20 °C. Colorless block crystals formed after several days. The supernatant liquid was removed by cannula, and the crystals were dried under vacuum to yield 0.140 g of product (69%). Anal. Calcd for $C_{32}H_{28}O_6F_8Zn_2$: C, 48.56; H, 3.57. Anal. Calcd. for $C_{24}H_{12}O_4F_8Zn_2$: C, 44.54; H, 1.87. Found: C, 42.53; H, 2.32. The inability to obtain a close match in elemental analysis is a result of the lability of the THF coordinated to the zinc center. ^1H NMR (C_5D_5N): δ 1.78 [m, 8 H{THF}], 3.74 [m, 8 H, {THF}], 6.45 [m, 4 H], 6.90 [t, 8 H{3,5-H}]. ^{13}C {H} NMR (C_5D_5N): δ 26.31 {THF}, 68.32 {THF}, 111.54−112.34 [m, {3,5-C_6H_3} {4-C_6H_3}], 145.38 [t, J_{C-F} = 15.6 Hz {ipso-C_6H_3}], 156.98 [dd, J_{C-Fl} = 235.95 Hz, J_{C-F2} = 18.61 Hz {2,6-C_6H_3}]. ^{19} F {H} NMR(C_5D_5N): δ −135.57.

Synthesis of $[(2,6\text{-Difluorophenoxide})_2Zn]_2(PCy_3)_2$, (2). A THF solution of 2,6-difluorophenol was added to a THF solution of $Zn[N(SiMe_3)_2]_2$ as described in the synthesis for complex **1**. The resulting clear colorless solution was stirred at room temperature for 30 min. A 5-mL THF solution of PCy_3 (0.145 g, 0.52 mmol) was subsequently added to the reaction mixture, and the resulting solution was allowed to stir for an additional 90 min. Colorless block crystals appeared upon cooling a concentrated THF solution (~3 mL) of the complex at −20 °C for several days. The supernatant liquid was removed by cannula, and the crystals were dried under vacuum to yield 0.181 g of product (58%). Anal. Calcd for $C_{60}H_{78}O_4F_8P_2Zn_2$: C, 59.65; H, 6.52. Found:

(5) Darensbourg, D. J.; Zimmer, M. S.; Rainey, P.; Larkins, D. L. *Inorg. Chem.* **2000**, *39*, 1578.
(6) Rokicki, A.; Kuran, W. *J. Macromol. Sci., Rev. Macromol. Chem.* **1981**, *C21*, 135.
(7) Super, M.; Berluche, E.; Costello, C.; Beckman, E. *Macromolecules* **1997**, *30*, 368.
(8) Cheng, M.; Lobkovsky, E. B.; Coates, G. W. *J. Am. Chem. Soc.* **1998**, *120*, 11018.
(9) Beckman, E. *Science* **1999**, *283*, 946.
(10) Darensbourg, D. J.; Zimmer, M. S. *Macromolecules* **1999**, *32*, 2137.
(11) Kunert, M.; Bräuer, M.; Klobes, O.; Görls, H.; Dinjus, E.; Anders, E. *Eur. J. Inorg. Chem.* **2000**, 1803.
(12) Darensbourg, D. J.; Niezgoda, S. A.; Draper, J. D.; Reibenspies, J. H. *Inorg. Chem.* **1999**, *38*, 1356.
(13) Burger, H.; Sawodny, W.; Wannaget, V. *J. Organomet. Chem.* **1965**, *3*, 113.
(14) SMART 1000 CCD; Bruker Analytical X-ray Systems: Madison, WI; 1999.
(15) SAINT-Plus, version 6.02; Bruker: Madison, WI; 1999.
(16) Sheldrick, G. SHELXS-86 Program for Crystal Structure Solution; Institut fur Anorganische Chemie der Universitat: Tammanstrasse 4, D-3400 Gottingen, Germany; 1986.
(17) Sheldrick, G. SHELXL-97 Program for Crystal Structure Refinement; Institut fur Anorganische Chemie der Universitat: Tammanstrasse 4, D-3400 Gottingen, Germany; 1997.
(18) SHELXTL, version 5.0; Bruker: Madison, WI; 1999.
(19) Darensbourg, D. J.; Zimmer, M. S.; Rainey, P.; Larkins, D. L. *Inorg. Chem.* **1998**, *37*, 2852.

Table 1. Crystallographic Data for Complexes **1**−**3** and **5**

	1	**2**	**3**	**5**
empirical formula	$C_{32}H_{28}F_8O_6Zn_2$	$C_{72}H_{102}F_8O_7P_2Zn_2$	$C_{32}H_{28}F_8K_2O_6Zn$	$C_{72}H_{102}F_8O_7P_2Cd_2$
FW	791.36	1424.14	803.2	1520.39
crystal system	triclinic	orthorhombic	monoclinic	triclinic
space group	*P*1(bar)	*Pna*2(1)	*C* 2/*c*	*P*1(bar)
V, Å^3	1554.4(4)	7000.8(8)	3772.6(6)	3498.1(8)
Z	2	4	4	2
a, Å	9.4696(15)	16.9185(11)	16.8412(16)	14.946(2)
b, Å	10.2093(16)	15.2890(10)	18.3146(17)	15.056(2)
c, Å	16.492(3)	27.0648(18)	13.5747(13)	15.609(2)
α, deg	78.116(3)	90.0	90.0	86.456(2)
β, deg	87.977(4)	90.0	115.707(2)	86.197(2)
γ, deg	85.147(4)	90.0	90.0	89.733(3)
T, K	110(2)	110(2)	110(2)	110(2)
d_{calcd}, g/cm^3	1.691	1.328	1.229	1.441
absorp coeff, mm^{-}1	3.379	0.803	0.939	2.050
unique reflections	7199	9409	4559	16009
observed reflections [$I > 2\sigma$**]**	2593	4369	3356	11 128
R,[a] % [$I > 2\sigma(I)$]	5.82	8.08	5.77	4.19
R_w,[a] %	9.11	18.71	15.51	10.11

[a] $R = \Sigma||F_o| - |F_c||/\Sigma F_o$. $R_w = \{[\Sigma w(F_o2 - F_c2)^2/[\Sigma w(F_o2)^2]\}^{1/2}$.

C, 59.64; H, 6.73. ^{1}H NMR (C_5D_6): δ 0.86−2.20 [m, 66 H, P(C_6H_{11})$_3$], 6.27 [m, 4 H], 6.80 [t, 8 H{3,5-H}]. ^{13}C {H} NMR (C_5D_5N): δ 27.31−32.66 P(C_6H_{11})$_3$, 111.69−112.12 [m, {3,5-C_6H_3} {4-C_6H_3}], 145.32 [t, J_{C-F} = 14.6 Hz {ipso-C_6H_3}], 156.94 [dd, J_{C-Fl} = 235.95 Hz, J_{C-F2} = 8.55 Hz {2,6-C_6H_3}]. ^{19}F{H} NMR(C_6D_6): δ −133.48 [bridging −$OC_6H_3F_2$], −127.38 [terminal −$OC_6H_3F_2$]. ^{31}P {H} NMR (C_6D_6): δ 9.576.

Synthesis of K$_2$[(2,6-Difluorophenoxide)$_4$Zn](THF)$_2$, (3). After the addition of 2,6-difluorophenol to Zn[N(SiMe$_3$)$_2$]$_2$, as in the preparation of **1**, and following an hour of stirring, a 5-mL THF solution of K(O-2,6-$F_2C_6H_3$) (0.174 g, 1.04 mmol) was added to the reaction mixture. The resulting solution was allowed to stir for an additional 90 min and then was concentrated to approximately 10 mL and placed in a freezer at −20 °C. Colorless block crystals formed after several days. The supernatant liquid was removed by cannula, and the crystals were dried under vacuum to yield 0.214 g of product (63%). Anal. Calcd for $ZnC_{24}H_{12}F_8O_4K_2$: C, 43.94; H, 1.85. Found: C, 43.64; H, 2.02. ^{1}H NMR (CD_3CN): δ 6.19 [m, 4 H], 6.62 [m, 8 H{3,5-H}]. ^{13}C {H} NMR (C_5D_5N): δ 111.27−111.81 [m, {3,5-C_6H_3} {4-C_6H_3}], 144.87 [t, J_{C-F} = 27.155 Hz {ipso-C_6H_3}], 156.69 [dd, J_{C-F1} = 233.84 Hz, J_{C-F2} = 9.05 Hz {2,6-C_6H_3}]. ^{19}F {H} NMR(CD_3CN): δ −136.782.

Synthesis of [(2,6-Difluorophenoxide)$_2$Cd]$_2$(THF)$_2$, (4). This complex was synthesized by a method similar to that described for **1** by adding a 5-mL THF solution of 2,6-difluorophenol (0.120 g, 0.92 mmol) to a 5-mL THF solution of Cd[N(SiMe$_3$)$_2$]$_2$ (0.20 g, 0.46 mmol). A white solid precipitated out immediately after the addition. This precipitate is assumed to be a dimeric species of bis-2,6-difluorophenoxide cadmium containing bridging phenoxides. This precipitate was washed several times with hexanes and dried under vacuum to yield 0.173 g (85%). Anal. Calcd for $C_{24}H_{12}O_4F_8Cd_2$: C, 38.89; H, 1.64. Found: C, 38.97; H, 1.69. ^{1}H NMR (C_5D_5N): δ 1.60[m, 8 H {THF}], 3.63 [m, 8 H, {THF}], 6.30 [m, 4 H], 6.94 [t, 8 H {3,5-H}. ^{13}C {H} NMR (C_5D_5N): δ 26.08 {THF}, 68.40 {THF}, 108.69 [t, {4-C_6H_3}], 112.2 [{3,5-C_6H_3}], 148.43 [t, J_{C-F} = 15.6 Hz {ipso-C_6H_3}], 157.91 [dd, J_{C-Fl} = 235.44 Hz, J_{C-F2} = 11.57 Hz {2,6-C_6H_3}]. ^{19}F{H} NMR-(C_5H_5N): δ −134.97.

Synthesis of [(2,6-Difluorophenoxide)$_2$Cd]$_2$(PCy$_3$)$_2$, (5). A 10-mL THF solution of 2,6-difluorophenol (0.120 g, 0.92 mmol) and PCy$_3$ (0.130 g, 0.46 mmol) were added concurrently to a 5-mL THF solution of Cd[N(SiMe$_3$)$_2$]$_2$ (0.20 g, 0.46 mmol), leading to a clear colorless solution which was stirred at room temperature for 2 h. The solution was then concentrated to approximately 8 mL and placed at −20 °C. Colorless block crystals formed after several days. The supernatant liquid was removed by cannula, and the crystals were dried under vacuum to yield 0.183 g of product (61%). Anal. Calcd for $C_{60}H_{78}O_4F_8P_2Cd_2$: C, 55.34; H, 6.05. Found: C, 55.14; H, 5.49. ^{1}H NMR (C_5D_6): δ 0.97−2.25 [m, 66 H, PC_6H_{11}], 6.18 [m, 4 H], 6.73 [t, 8 H{3,5-H}]. ^{13}C {H} NMR (C_5D_5N): δ 27.26−32.65 (PC_6H_{11}), 108.86 [t, {4-C_6H_3}], 111.94 [m, {3,5-C_6H_3}], 148.16 [t, J_{C-F} = 15.6 Hz {ipso-C_6H_3}], 157.83 [dd, J_{C-F1} = 235.45 Hz, J_{C-F2} = 11.07 Hz {2,6-C_6H_3}]. ^{19}F {H} NMR-(C_6D_6): δ −134.74. ^{31}P {H} NMR (C_6D_6): δ 30.63 [dd, J^{113}_{Cd-P} = 2508 Hz, J^{111}_{Cd-P} = 2390 Hz].

Synthesis of [(2,6-Dichlorophenoxide)$_2$Zn]$_2$(THF)$_2$, (6). A 5-mL THF solution of 2,6-dichlorophenol (0.170 g, 1.04 mmol) was added to a 5-mL THF solution of Zn[N(SiMe$_3$)$_2$]$_2$ (0.20 g, 0.52 mmol), leading to a clear colorless solution which was stirred at room temperature for 2 h. The product was isolated by precipitation with hexanes, and the supernatant liquid was removed by cannula. The solid was then vacuumed to dryness, yielding 0.199 g (69%). Anal. Calcd for $C_{24}H_{12}O_4Cl_8Zn_2$·(THF)$_2$: C, 41.64; H, 3.06. Anal. Calcd for $C_{24}H_{12}O_4Cl_8Zn_2$: C, 37.01; H, 1.56. Found: C, 37.29; H, 2.18. As with **1**, THF lability causes an inaccurate match in the elemental analysis. ^{1}H NMR (C_5D_5N): δ 1.86 [m, 8 H {THF}], 3.61 [m, 8 H, {THF}], 6.47 [t, 4 H {4-H}], 7.35 [d, 8 H{3,5-H}]. ^{13}C {H) NMR (C_5D_5N): δ 26.31 {THF}, 68.32 {THF}, 115.42 [s, {4-C_6H_3}], 125.74 [s, {3,5-C_6H_3}], 128.90 [s, {2,6-C_6H_3}], 158.52 [s, {ipso-C_6H_3}].

Synthesis of [(2,6-Dibromo-4-methylphenoxide)$_2$Zn]$_2$(THF)$_2$, (7). A 5-mL THF solution of 2,6-dibromo-4-methylphenol (0.275 g, 1.04 mmol) was added to a 5-mL THF solution of Zn[N(SiMe$_3$)$_2$]$_2$ (0.20 g, 0.52 mmol), leading to a clear colorless solution which was stirred at room temperature for 2 h. The product was isolated by precipitation with hexanes, and the supernatant liquid was removed by cannula. The solid was then vacuumed to dryness, yielding 0.275 g (75%). Anal. Calcd for $C_{36}H_{40}O_6Br_8Zn_2$: C, 32.39; H, 2.72. Found: C, 30.90; H, 2.53. ^{1}H NMR (C_5D_5N): δ 1.61 [m, 4 H{THF}], 2.02 [s, 12 H{-CH_3}], 3.64 [m, 4 H, {THF}], 7.30 [s, 8 H{3,5-H}]. ^{13}C {H} NMR (C_5D_5N): δ 20.05 [s, {-CH_3}], 26.31 {THF}, 68.32 {THF}, 115.72 [s, {4-C_6H_3}], 123.01 [s, {3,5-C_6H_3}], 126.21 [s,{2,6-C_6H_3}], 157.29 [s, {ipso-C_6H_3}].

X-ray Crystallography. A Bausch and Lomb 10× microscope was used to identify suitable colorless crystals of **1**−**3** and **5** from a representative sample of crystals of the same habit. The representative crystal was coated in a cryogenic protectant (i.e., mineral oil, paratone, or apezeon grease) and was then fixed to a glass fiber, which in turn was fashioned to a copper mounting pin. The mounted crystals were then placed in a cold nitrogen stream (Oxford) maintained at 110 K on a Bruker SMART 1000 three-circle goniometer.

Crystal data and details of data collection for the complexes are provided in Table 1. The X-ray data were collected on a Bruker CCD diffractometer and covered more than a hemisphere of reciprocal space by a combination of three sets of exposures; each exposure set had a different φ angle for the crystal orientation, and each exposure covered 0.3° in ω. The crystal-to-detector distance was 4.9 cm. Crystal decay was monitored by repeating the data collection for 50 initial frames at the end of the data set and analyzing the duplicate reflections; crystal decay was negligible. The space group was determined on the basis of systematic absences and intensity statistics.[14]

The structures were solved by direct methods. Full-matrix least-squares anisotropic refinement for all non-hydrogen atoms yielded R_F and wR_{F^2} values as indicated in Table 1 at convergence. Hydrogen atoms were place in idealized positions with isotropic thermal parameters fixed 1.2 or 1.5 times the value of the attached atom. Neutral atom scattering factors and anomalous scattering factors were taken from the International Tables for X-ray Crystallography, Vol. C.

For the title compound: data reduction, SAINTPLUS (Bruker[15]); program(s) used to solve the structure, SHELXS-86 (Sheldrick[16]); program(s) used to refine the structure, SHELXL-97 (Sheldrick[17]); program(s) used for molecular graphics, SHELXTL version 5.0 (Bruker[18]); software used to prepare material for publication, SHELXTL version 5.0 (Bruker[18]).

Solid-State ^{113}Cd NMR. The solid-state NMR spectra were acquired utilizing a Bruker MSL 300 superconducting spectrometer equipped with a magnet operating at 7.05 T (Larmor frequency of 66.546 MHz for ^{113}Cd). The samples were ground and packed into zirconium oxide rotors with Kel-F end caps for use in a 7-mm supersonic probe from Bruker. Spinning speeds were regulated by a Bruker spin rate controller. All chemical shifts and tensor elements were referenced to an external sample of 0.1 M $Cd(C1O_4)_2$ in D_2O solution at 25 °C, with positive shifts denoting movement of resonances to lower shielding. $Cd(NO_3)_2 \cdot 4H_2O$ was used as a secondary standard relative to the cadmium perchlorate solution in D_2O to account for the cross polarization (CP) with proton decoupling. The recycle delay used was 15 s, with a 1 H $7\pi/2$ pulse width, 5.25 μs, and a contact time of 15 ms for all samples. Principal elements of the shielding tensor were extracted utilizing WINFIT software package from Bruker Instruments running on a Adosea pentium personal computer.

High-Pressure Copolymerization of CO_2 with Cyclohexene Oxide. A sample of the active catalyst (0.100 g) was dissolved in 20.0 mL of cyclohexene oxide. The solution was loaded via an injection port into a 300-mL stainless steel Parr autoclave which had previously been dried overnight under vacuum at 80 °C. The reactor was pressurized to 600 psi with $C0_2$ and heated to 80 °C, which increased the pressure to 750−800 psi, and left to react between 24 and 48 h. After 24−48 h of reaction time, the reactor was cooled and opened, and the viscous/solid mixture was isolated by dissolution in CH_2Cl_2 and precipitated out in MeOH. The polymer was analyzed by ^{1}H and ^{13}C NMR spectroscopy and by GPC measurements. We have determined physical and mechanical properties of the poly(cyclohexenylene carbonate) polymer produced herein, as well as a comparison of similar characteristic of it with the widely applied bisphenol A-polycarbonate polymer. These latter experiments were carried out in collaboration with the research group of Dr. Cor Koning at DSM, The Netherlands. This work is being published elsewhere.

High-Pressure Copolymerization of CO_2 with Propylene Oxide. A 0.100-g amount of active catalyst was dissolved in 20.0 mL of propylene oxide. The resulting solution was added through the injection port to a predried 300-mL autoclave, and the reactor was pressurized to 600 psi with CO_2. The reactor was heated at 55 °C, raising the pressure to 650−700 psi, for 48 h. After this period of time, the reaction mixture was diluted with CH_2Cl_2 (1:10) and analyzed by infrared spectroscopy in the ν(CO) region.

High-Pressure Terpolymerization of CO_2 with Propylene Oxide and Cyclohexene Oxide. A 0.100-g amount of active catalyst was dissolved in a solution composed of 10.0 mL (∼50 mol %) of cyclohexene oxide and 7.0 mL (∼50 mol %) of propylene oxide. The resulting solution was added through the injection port of a 300-mL predried autoclave, and the reactor was pressurized to 600 psi with CO_2. The reactor was then heated to 55 °C, raising the pressure to 650−700 psi, for between 24 and 48 h. After this period of time, the reactor was opened, and the viscous/solid mixture was dissolved in CH_2Cl_2 and precipitated out in MeOH. The polymer was analyzed by ^{1}H and ^{13}C NMR spectroscopy and by DSC measurements.

Results and Discussion

Synthesis, Spectral, and Structural Characterization of Dimeric Zinc and Cadmium Phenoxides. The dimeric zinc phenoxide derivatives were synthesized and isolated in purified yields of >60% by the general synthetic route described by Caulton and co-workers,[1] and by previous work in our laboratories,[3,4] for the synthesis of a large variety of monomeric $(ArO)_2Zn(base)_2$ complexes. The reactions, depicted specifically in eq 1 for the 2,6-difluorophenol derived product, were carried out in THF solution and employing purified starting materials. Although vacuum-dried samples of complex **1** exhibited varying levels of THF content as indicted by C,H elemental analysis, ^{1}H NMR of the isolated complex revealed the presence of one THF molecule per zinc. Crystals of complex **1** suitable for X-ray analysis were obtained from a cooled (−20 °C) concentrated solution of the complex in THF.

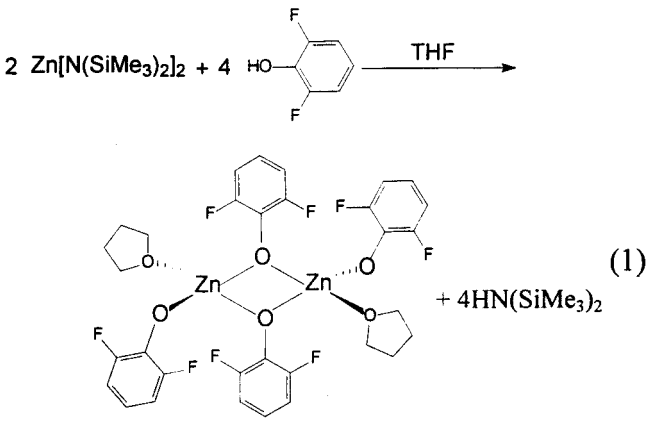

(1)

1

Subsequent reaction of complex **1** with two equivalents of the sterically encumbering basic tertiary phosphine, PCy_3, at ambient temperature resulted in the formation of complex **2**, in which the THF ligands are simply displaced by the better donor phosphine ligands. On the other hand, the addition of four equivalents of $K(O\text{-}2,6\text{-}F_2C_6H_3)$ in THF to complex **1** led to disruption of the dimeric structure with concomitant production of the monomeric dianion, **3**. In this instance, the proclivity of the nonbulky phenoxide to bridge two zinc centers is overcome by the addition of strong nucleophiles. These processes are represented in Scheme 1. Colorless crystals suitable for X-ray crystallographic studies of both derivatives, **2** and **3**, were readily obtained from concentrated, cooled (−20 °C) solutions of the respective complex in THF.

The cadmium analogue of complex **1** was synthesized in a manner similar to that described for the zinc derivative. However, upon adding 2,6-difluorophenol to $Cd[N(SiMe_3)_2]_2$, the product $[Cd(O\text{-}2,6\text{-}F_2C_6H_3)_2 \cdot THF]_2$, **4**, immediately precipitated from the THF solution. Nevertheless, complex **4** is concluded to be dimeric, as evident by ^{1}H NMR in C_5D_5N and elemental analysis, which show 1 equiv of THF per cadmium center. Upon addition of PCy_3 simultaneously with the phenol to the cadmium amide in THF, the complex formed remains in solution to afford the analogue to complex **2**, $[Cd(O\text{-}2,6\text{-}F_2C_6H_3)_2 \cdot PCy_3]_2$ (**5**). Well-formed crystals of this latter derivative were obtained from a cooled, concentrated THF solution of **5**.

In addition, it was possible to prepare the corresponding chloro- and bromophenolate derivatives of complex **1** in a similar manner. However, after several attempts at crystallization, it has not thus far been possible to obtain crystals suitable for definitive X-ray structure determinations. Again, ^{1}H NMR and elemental analysis imply that these species are also dimeric, in that one equivalent of THF per zinc metal was found. Recall that monomeric zinc phenoxides exhibit 2 equivs of THF per zinc center.

Scheme 1

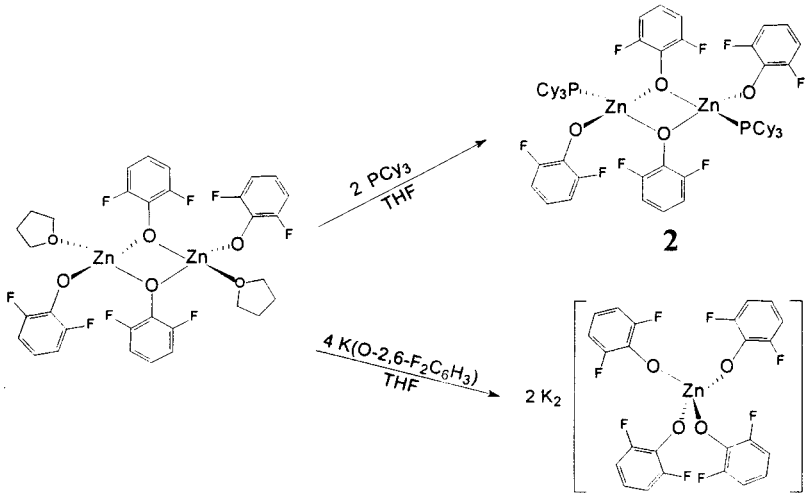

3

Complexes **1**−**3** and **5** have been characterized in the solid state by X-ray crystallography, and a list of selected bond lengths and angles is provided in Table 2. In the crystallographic independent unit of complexes **1** and **5,** two half molecules of **1** and **5** were found; therefore, for each complex, quite similar bond distances and angles are separately compiled in Table 2 for the two independently generated molecules. Complex **1** crystallized from THF as a dimer in which the zinc centers are coordinated in distorted tetrahedral geometry, each containing two bridging phenoxides and a terminal phenoxide and THF ligand. Figure 1 displays a thermal ellipsoid rendering of **1**, along with a partial atom-labeling scheme for one of the molecules generated from the two half molecules in the unit cell (See Supporting Information for the other labeling scheme). Because the molecular parameters are so similar, only those for one of the independently generated molecules in the unit cell will be discussed. The structure of **1** consists of a planar arrangement of the zinc atoms and the oxygen atoms of the bridging phenoxide ligands which form a parallelogram with an O−Zn−O bond angle of 80.07(19)° and a Zn−O−Zn bond angle of 99.93(19)°. The Zn−O bond lengths for the bridging phenoxide ligands average 1.992(4) Å, in which the terminal phenoxide Zn−O bond length is over 0.1 Å shorter at 1.869(4) Å. The distance between the metal centers (Zn···Zn) in the dimer is 3.059 Å. By way of comparison, the parallelogram formed by the two bridging 2,6-di-*tert*-butylC_6H_3O and two zinc atoms of the previously reported dimer, $[Zn(O\text{-}2,6\text{-}t\text{-}Bu_2C_6H_3)_2]_2$, where the zinc centers are coordinated in a distorted trigonal planar geometry, is more rectangular, with an average O−Zn−O angle of 82.4(1)°. This, coupled with the shorter average Zn−O bond length for the more basic bridging phenoxide of 1.961(1) Å, places the metal centers closer, with a Zn···Zn distance of 2.9484(6) Å.[11] The two THF ligands in complex **1**, with Zn−O bond lengths of 2.003(4) Å, are arranged in a trans configuration. The average Zn−O−C(aryl) bond angles are 129.7 and 124.0° for bridging and terminal phenoxides, respectively.

Interestingly, there are several short Zn···F nonbonding distances in **1**, with those involving the fluorine atoms of the two bridging phenoxides being the shorter. That is, the Zn(1)···F(2) and Zn···F(1A) separations were found to be 2.837 and 2.768 Å, respectively. Comparable distances in the other molecule, that is, Zn(2)···F(6A), were determined to be 2.746 and 2.7019 Å, respectively. This is illustrated in Figure 2 for the closest Zn···F interaction comprising F(1A), which leads to an incipient planar five-membered chelate ring. These separations are slightly shorter than the nonbonded van der Waals internuclear distance of 2.86 Å. The distances for the nearest fluorine atom of the terminal phenoxide to the zinc center (Zn(1)···F(3) and Zn(2)···F(7)) are 2.961 Å and 2.728 Å.

As indicated in Figure 3, which represents the thermal ellipsoid drawing of complex **2**, and in Table 2, there is little perturbation to the dimeric unit of complex **1** upon replacing the THF donor ligands with the sterically encumbering, basic phosphine, PCy_3. As was the case for the THF ligands, the tricyclohexylphosphine ligands are accommodated in a trans configuration. The average Zn−P bond distance of 2.410(4) Å is slightly shorter than that of 2.433(2) Å, which is found in the monomeric $Zn(O\text{-}2,6\text{-}t\text{-}Bu_2C_6H_3)_2{\cdot}PCy_3$ derivative.[5,19] In complex **2**, because of the bulky phosphine ligands, the fluorine atoms of the terminal phenoxide ligands are significantly closer to the metal centers, with Zn(1)···F(7) and Zn(2)···F(1) separations of 2.840 and 2.856 Å, respectively. The bridging phenoxides provide Zn(1)···F(4) and Zn(2)···F(6) distances of 3.191 and 3.158 Å. Three molecules of THF are found in the crystal lattice per independent unit.

Complex **3**, which results from the addition of the strong nucleophile, $O\text{-}2,6\text{-}F_2C_6H_3^-$ to **1,** leads to a disruption of the dimeric structure by formation of a monomeric tetrakisphenoxide zinc dianion of distorted tetrahedral geometry. Figure 4 contains a thermal ellipsoid representation of complex **3**. Two of the phenoxide ligands are bound to zinc with Zn−O bond lengths of 1.949(3) Å, whereas the corresponding other two Zn−O bond lengths are slightly longer at 1.974(3) Å. The O−Zn−O bond angles range from 97.1 to 117.6°, with an average value of 109.7°. Previously, we reported trisphenoxide derivatives of zinc and cadmium which were produced by the addition of the sterically demanding phenoxide, $KO\text{-}2,6\text{-}t\text{-}Bu_2C_6H_3$, to the monomeric $M(O\text{-}2,6\text{-}t\text{-}Bu_2C_6H_3)_2{\cdot}2THF$ derivatives.[20] The structures of these anions are trigonal planar, and the potassium cations are surrounded by six THF molecules. On the other hand, in complex **3**, the potassium cations exhibit interaction with both fluorine atoms (K···F = 2.723(3) Å) and THF molecules.

(20) Darensbourg, D. J.; Niezgoda, S. A.; Draper, J. D.; Reibenspies, J. H. *Inorg. Chem.* **1999**, *38*, 1356.

Table 2. Selected Bond Distances (Å) and Bond Angle (deg) for Complexes **1**−**3**, and **5**[a,b]

	Complex **1**		
Zn(1)−O(1)	1.986(4)	Zn(1)−O(lA)	1.997(4)
Zn(1)−O(2)	1.869(4)	Zn(1)−O(3)	2.003(4)
Zn(1)−O(l)−Zn(1A)	99.93(19)	O(1)−Zn(1)−O(lA)	80.07(19)
O(2)−Zn(1)−O(1)	131.3(2)	O(2)−Zn(1)−O(1A)	122.31(17)
Zn(1)−O(1)−C(aryl)	129.7(4)	Zn(1)−O(2)−C(aryl)	124.0(4)
Zn(2)−O(4)	1.980(4)	Zn(2)−O(4A)	1.986(4)
Zn(2)−O(5)	1.877(4)	Zn(2)−O(6)	2.008(4)
Zn(2)−O(4)−Zn(2A)	101.34(19)	O(4)−Zn(2)−O(4A)	78.66(19)
O(5)−Zn(2)−O(4)	124.81(19)	O(5)−Zn(2)−O(4A)	136.89(17)
Zn(2)−O(4)−C(aryl)	128.2(4)	Zn(2)−O(5)−C(aryl)	125.1(4)
	Complex **2**		
Zn(1)−O(1)	2.001(8)	Zn(1)−O(3)	1.916(9)
Zn(1)−O(2)	2.013(9)	Zn(1)−P(2)	2.419(4)
Zn(2)−O(1)	2.006(9)	Zn(2)−O(2)	2.022(8)
Zn(2)−O(4)	1.878(8)	Zn(2)−P(1)	2.401(4)
Zn(1)−O(2)−Zn(2)	99.3(4)	Zn(1)−O(1)−Zn(2)	100.3(4)
O(1)−Zn(1)−O(2)	80.4(3)	O(1)−Zn(2)−O(2)	80.1(3)
O(1)−Zn(2)−O(4)	124.6(4)	O(1)−Zn(1)−P(2)	114.7(3)
O(2)−Zn(1)−P(2)	117.1(3)	Zn(1)−O(1)−C(aryl)	131.8(8)
Zn(1)−O(2)−C(aryl)	128.0(8)	Zn(2)−O(1)−C(aryl)	127.6(8)
Zn(2)−O(2)−C(aryl)	131.8(8)	O(2)−Zn(1)−O(3)	123.6(3)
O(1)−Zn(2)−P(1)	117.4(2)	O(2)−Zn(2)−P(1)	114.8(3)
	Complex **3**		
Zn(1)−O(1)	1.949(3)	Zn(1)−O(2)	1.974(3)
O(1)−Zn(1)−O(lB)	114.49(17)	O(1)−Zn(1)−O(2B)	97.10(11)
O(2)−Zn(1)−O(1B)	97.10(11)	O(1)−Zn(1)−O(2)	117.58(11)
Zn(1)−O(2)−C(aryl)	121.6(2)	O(2)−Zn(1)−O(2B)	114.34(15)
Zn(1)−O(1)−C(aryl)	132.8(3)		
	Complex **5**		
Cd(1)−O(1)	2.222(2)	Cd(1)−O(lA)	2.255(2)
Cd(1)−O(2)	2.124(2)	Cd(1)−P(1)	2.5426(10)
O(1)−Cd(1)−O(lA)	77.17(10)	Cd(l)−O(1)−Cd(lA)	102.83(9)
O(2)−Cd(1)−O(1)	116.00(10)	O(2)−Cd(1)−O(lA)	118.25(10)
Cd(1)−O(1)−C(aryl)	126.3(2)	Cd(1)−O(2)−C(aryl)	126.4(2)
O(1)−Cd(1)−P(1)	124.15(7)	O(2)−Cd(1)−P(1)	106.88(8)
O(1A)−Cd(1)−P(1)	112.32(7)		
Cd(2)−O(3)	2.244(2)	Cd(2)−O(3A)	2.229(3)
Cd(2)−O(4)	2.127(2)	Cd(2)−P(2)	2.5470(10)
O(3)−Cd(2)−O(3A)	77.66(10)	Cd(2)−O(3)−Cd(2A)	105.24(10)
O(4)−Cd(2)−O(3)	129.29(10)	O(4)−Cd(2)−O(3A)	123.21(10)
Cd(2)−O(3)−C(aryl)	128.8(2)	Cd(2)−O(4)−C(aryl)	128.1(2)
O(3)−Cd(2)−P(2)	114.79(7)	O(4)−Cd(2)−P(2)	102.98(8)
O(3A)−Cd(2)−P(2)	119.08(7)		

[a] Estimated standard deviations are given in parentheses. [b] Symmetry-generated atoms designated by (number A).

The cadmium analogue of complex **2** is also dimeric in the solid state,that is, $[Cd(O\text{-}2,6\text{-}F_2C_6H_3)_2 \cdot PCy_3]_2$ (**5**). A thermal ellipsoid representation of complex **5** is shown in Figure 5 for one of the independently generated molecules in the unit cell. Because molecular parameters in the two independent molecules are so similar (see Table 2), we will discuss only one here. Three molecules of THF are found in the crystal lattice per independent unit. The parallelogram formed by the two cadmium centers and the bridging oxygen atoms of the phenoxide ligands has an O−Cd−O angle smaller by ∼3° (77.17(10)°) and a Cd−O−Cd angle larger by ∼3° (102.83(9)°) than those of complex **2**. The nonbonding Cd···Cd separation of 3.499 Å, as compared to 3.059 Å for the zinc analogue, is consistent with the difference in the radii of cadmium vs zinc. The Cd−O bridging phenoxide bond lengths average 2.239(2) Å, whereas the terminal Cd−O bond distances are 2.124(2) Å. By way of contrast to complex **2**, the Cd−P bond length at 2.5426(9) Å is slightly longer than that in the monomeric species $Cd(O\text{-}2,6\text{-}t\text{-}Bu_2C_6H_3)_2 \cdot PCy_3$ of 2.5274(12) Å, and the shortest Cd···F nonbonding distances are

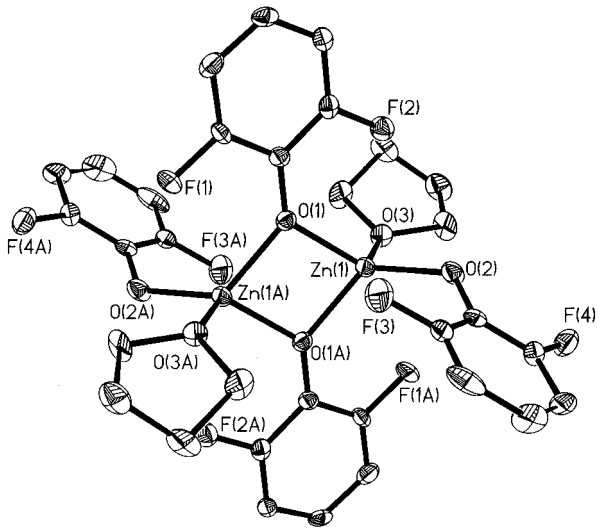

Figure 1. Thermal ellipsoid representation of complex **1**.

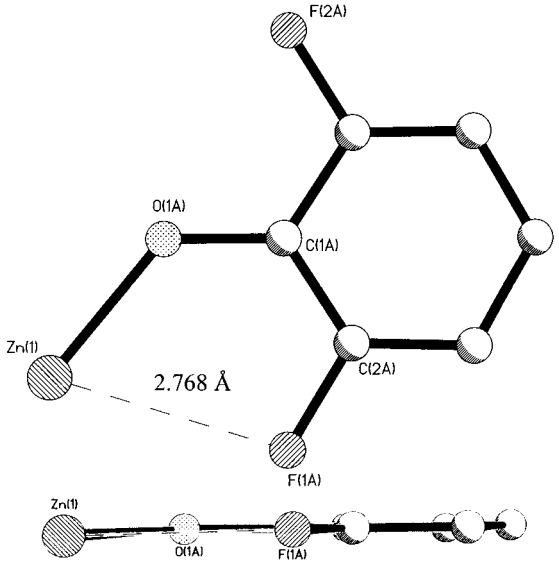

Figure 2. Closet Zn···F interaction in complex **1**. Insert illustrates planarity of the incipient five-membered chelate ring.

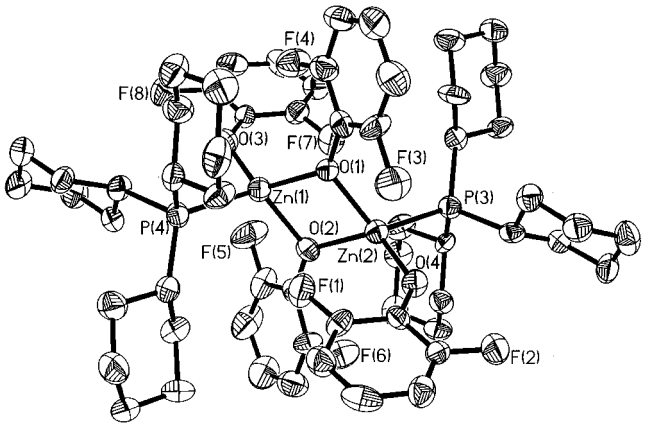

Figure 3. Thermal ellipsoid representation of complex **2**.

to the fluorine atoms of the bridging phenoxides at 2.858 Å. Again, this latter separation is shorter than the nonbonded Cd···F van der Waals internuclear distance of 3.05 Å.

In addition, these zinc and cadmium bisphenoxide derivatives readily lend themselves to characterization in solution via multinuclear NMR spectroscopy. For example, the ^{19}F NMR

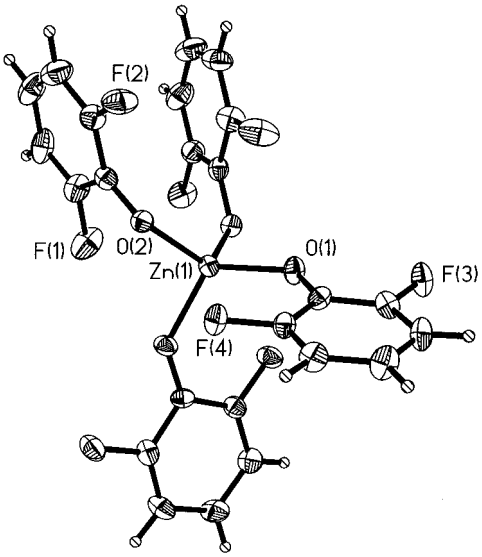

Figure 4. Thermal ellipsoid representation of the anion of complex **3**.

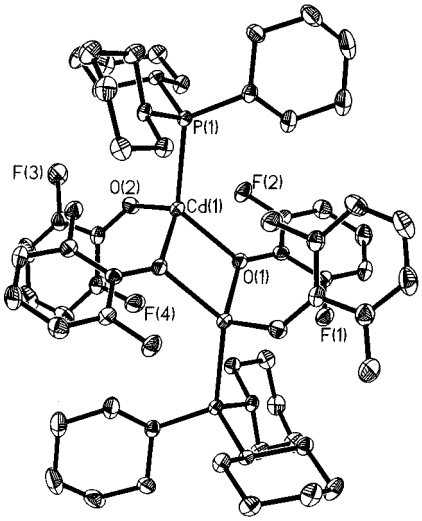

Figure 5. Thermal ellipsoid representation of complex **5**.

spectrum of complex **2** in C_6D_6 is consistent with its solid-state structure, exhibiting two resonances of equal intensity that correspond to bridging and terminal phenoxide ligands at −133.5 and −127.4 ppm which are shifted upfield from the free phenol. Further, the ^{31}P NMR spectrum of complex **2** in C_6D_6 displayed a small upfield shift from that of free PCy_3, going from 10.6 ppm for unbound PCy_3 to 9.58 ppm in the bound complex. Both bound and free ^{31}P resonances are sharp at ambient temperature for complex **2** in the presence of 0.1 equiv of free PCy_3 (vide infra). Conversely, the dimeric nature of the solid-state structures of the dichloro- and dibromophenolate analogues of complex **1** (complexes **6** and **7**) is confirmed by the ^{1}H NMR spectra of these derivatives in C_5D_5N, which showed that 1 equiv of THF was bound per zinc center prior to dissolution in C_5D_5N, whereas monomeric zinc bisphenoxides show 2 equivs of bound THF per zinc center. On the other hand, complex **1** appears to be monomeric in the strongly coordinating solvent C_5D_5N, with only one ^{19}F resonance being observed at −136.8 ppm. Presumably because of their close similarity, complexes **6** and **7** are also monomeric in C_5D_5N solution.

The cadmium analogue of complex **1**, $[Cd(O\text{-}2,6\text{-}F_2C_6H_3)_2\cdot THF]_2$ (**4**), is soluble only in strong bases such as pyridine, in which it is most likely dissociated into monomeric species. That is, complex **4** dissolved in C_5D_5N exhibits a single resonance in the ^{19}F NMR spectrum at 134.97 ppm, which is indicative of only terminal phenoxide ligands. On the other hand, the isotropic ^{113}Cd chemical shift of **4** obtained in the solid state at 9.26 ppm (chemical shift anisotropy and asymmetry parameter of −245 and 0.20 ppm, respectively) is consistent with a dimeric structure similar to that of the zinc derivative, that is, a cadmium center containing 4 oxygen donor ligands.[21]

The CP/MAS solid-state ^{113}Cd NMR spectrum of complex **5**, $[Cd(O\text{-}2,6\text{-}F_2C_6H_3)_2\cdot PCy_3]_2$, displays an isotropic shift (σ_{iso}) of 252.6 ppm with $J^{113}_{Cd-P} = 2297$ Hz. The chemical shift anisotropy and asymmetry parameter were determined to be −253 and 0.70 ppm, respectively. The solid-state ^{31}P NMR spectrum of **5** was composed of a resonance at 26.5 ppm with coupling to cadmium. However, due to limitations on spinning speeds, the resonances due to ^{111}Cd−^{31}P and ^{113}Cd−^{31}P coupling could not be distinguished, thereby not allowing for an accurate determination of coupling constants. The ^{113}Cd NMR spectrum of complex **5** in THF solution is similar to that obtained in the solid state, displaying a chemical shift (δ) of 232.2 ppm with $J^{113}_{Cd-P} = 2480$ Hz at −80 °C. A complex cadmium spin−spin coupling pattern to the fluorine nuclei of two types of phenoxide ligands was also observed, with $J^{113}_{Cd-F} \approx 66$ Hz. The ^{31}P resonance of complex **5** in THF solution appears at 30.7 ppm, with a ^{113}Cd−^{31}P coupling constant of 2508 Hz. This resonance is significantly downfield from that of free PCy_3 and is slightly upfield from the value for the monomer $Cd(O\text{-}2,6\text{-}t\text{-}Bu_2C_6H_3)_2\cdot PCy_3$ ($\delta = 31.3$ ppm with $J_{Cd-P} = 2274$ Hz).[19] Two ^{19}F resonances were noted in THF solution at −80 °C, −135.8 and −136.7 ppm for bridging and terminal phenoxide ligands.

Curiously, the ^{113}Cd, ^{31}P, and ^{19}F NMR spectra of complex **5** in solution were very dependent on the presence of small quantities of free PCy_3 impurities in the sample. This, in turn, accounts for the temperature dependence of these NMR spectra under these conditions. For example, in these instances, the ^{31}P NMR spectrum at ambient temperature is slightly broadened, and it is not possible to differentiate between the ^{113}Cd−P and ^{111}Cd−P coupling constants. However, when the temperature is lowered, the resonance due to complex **5** sharpens and clearly displays coupling to both cadmium isotopes (see Figure 6). Simultaneously, a second minor resonance appears upfield, around 24 ppm, which exhibits Cd−P coupling. Over this same temperature range (ambient to −80 °C) the ^{19}F NMR spectra proceed from a single resonance at −135.4 ppm to two principal signals of equal intensity at −135.8 and −136.7 ppm, with the former displaying some unresolved coupling to cadmium, which we assign to the bridging phenoxide ligand. Similarly, under these conditions (small excess of PCy_3 and ambient to −80 °C), the ^{113}Cd NMR spectrum shifts from a doublet centered at 218.8 ppm to one centered at 232.2 ppm.

The identity of the minor cadmium phosphine species ($\delta^{31}_P = 22.4$ ppm with J^{111}_{Cd-P} and $J^{113}_{Cd-P} = 1590$ and 1665 Hz at −80 °C, respectively) present in samples of complex **5** containing small quantities of free PCy_3 becomes apparent when excess PCy_3 is added to **5**. That is, the addition of 6 equivs of PCy_3 to a sample of pure $[Cd(O\text{-}2,6\text{-}F_2C_6H_3)_2\cdot PCy_3]_2$ (**5**) resulted in a ^{31}P NMR spectrum at ambient temperature which consisted of broad, weak signals due mainly to **5** and free PCy_3. When the sample was cooled incrementally, the ^{31}P resonance due to complex **5** initially sharpened and decreased in intensity with concomitant increases in intensity of the signals at ∼24 ppm (which displays unresolved ^{111}Cd and ^{113}Cd coupling) and that of free PCy_3. Finally, at −80 °C the latter two resonances are

(21) Darensbourg, D. J.; Niezgoda, S. A.; Draper, J. D.; Reibenspies, J. H. *J. Am. Chem. Soc.* **1998**, *120*, 4690.

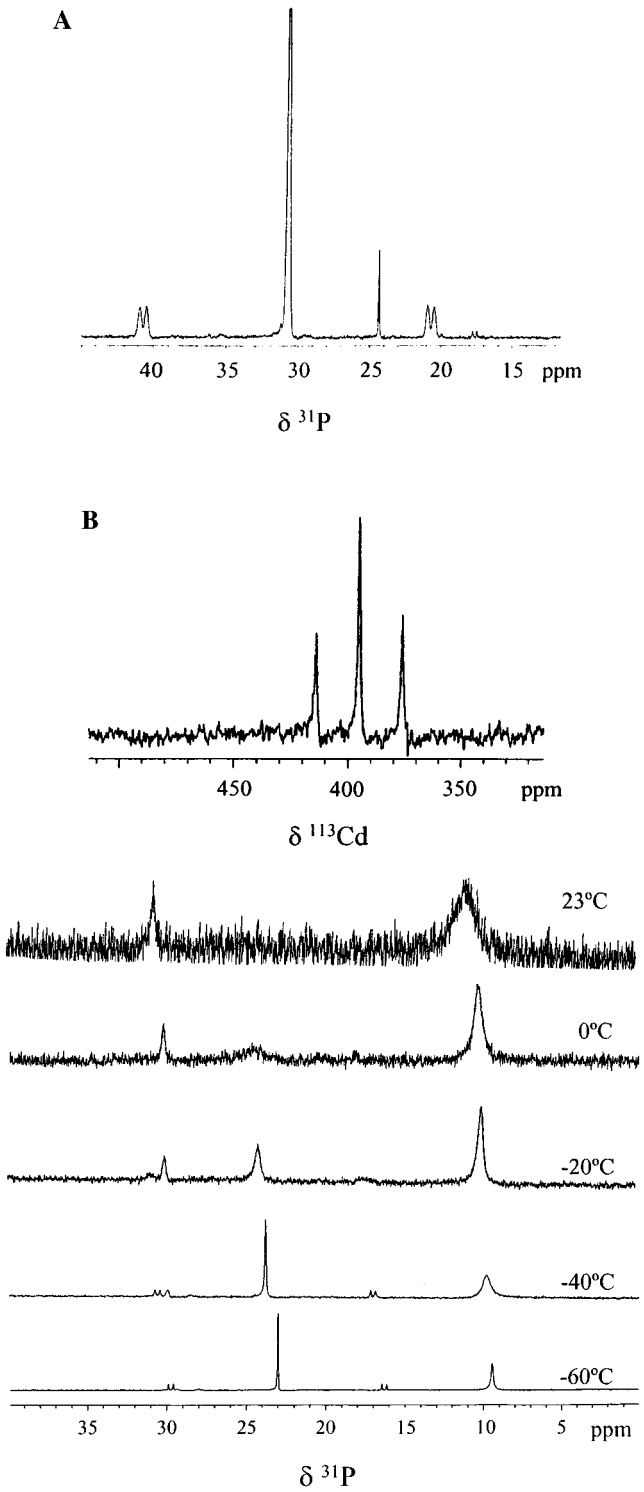

Figure 6. Variable-temperature ^{31}P NMR spectra of complex **5** in the presence of 6 equivs of PCy_3. Insert A shows ^{31}P NMR spectrum of complex **5** with small quantities of free PCy_3 at −60 °C. Insert B represents the ^{113}Cd NMR spectrum of **5** in the presence of 6 equivs of PCy_3 at −40 °C.

sharp and are the only ^{31}P signals present in the spectrum. The ^{113}Cd NMR spectrum of this sample exhibits two broad resonances centered at ∼220 and ∼360 ppm at ambient temperature which ultimately are converted to a triplet centered at 395.1 ppm, with $J^{113}_{Cd-^{31}P}$ value of 1678 Hz at −40 °C. These observations are summarized in Figure 6. At the same time, the sample displays only one ^{19}F resonance in the ^{19}F NMR spectrum at −137.5 ppm. This spectral behavior is readily explained by a rapid equilibrium process, as described in eq 2, which is shifted far to the right as the temperature is lowered. This is consistent, as well, with the conclusion based on the spectrum of complex **4** when it is dissolved in the strongly coordinating solvent, C_5D_5N (i.e., eq 3).

Table 3. Catalytic Activity for the Copolymerization of Carbon Dioxide and Cyclohexene Oxide[a]

catalyst	turnover no (g polym/g Zn)	turnover freq (g poly/g Zn/hr)
$[Zn(O\text{-}2,6\text{-}F_2C_6H_3)_2\cdot THF]_2$[b] **1**	790	16.5
$[Zn(O\text{-}2,6\text{-}Cl_2C_6H_3)_2\cdot THF]_2$ **6**	539	11.2
$[Zn(O\text{-}2,6\text{-}Br_2, 4\text{-}MeC_6H_2)_2\cdot THF]_2$ **7**	329	7.2

[a] Catalyst loading (0.100 g), 20.0 mL of cyclohexene oxide, CO_2 at ambient temperature 41.3 bar. Reaction conditions: 80 °C at a total pressure of 55 bar. [b] Molecular weight distribution of copolymer: absolute M_n and M_w = 42 000 and 252 000 g/mole, or a PDI = 6.0.

$$[Cd(O\text{-}2,6\text{-}F_2C_6H_3)_2\cdot PCy_3]_2 + \text{excess } PCy_3 \rightleftharpoons 2Cd(O\text{-}2,6\text{-}F_2C_6H_3)_2(PCy_3)_2 \quad (2)$$

$$[Cd(O\text{-}2,6\text{-}F_2C_6H_3)_2\cdot THF]_2 + \text{excess } C_5H_5N \rightleftharpoons 2Cd(O\text{-}2,6\text{-}F_2C_6H_3)_2(C_5H_5N)_2 \quad (3)$$

By way of contrast, in the presence of sterically encumbering phenoxides such as 2,6-$Ph_2C_6H_3O^-$ and 2,6-*t*-$Bu_2C_6H_3O^-$, the monomeric cadmium derivatives have been fully characterized as monophosphine complexes of PCy_3 which exhibit no exchange with free PCy_3 in solution. This is indicative of the bisphosphine complex's being inaccessible in these instances. That is, rapid phosphine exchange occurs via an associative pathway. Conversely, these bulky phenoxide derivatives of cadmium in the presence of smaller phosphines, such as PMe_3, readily form bisphosphine complexes. Indeed, Cd(O-2,6-*t*-$Bu_2C_6H_3)_2(PMe_3)_2$ has been characterized in the solid state by X-ray crystallography.[22] Furthermore, in these cases, the bisphenoxide complexes were shown to be in rapid equilibrium with free phosphine and the monophosphine derivatives, with the equilibrium position being shifted in favor of the bisphosphine derivative at low temperature.

Copolymerization Reactions of Epoxides and Carbon Dioxide. Complex **1**, $[Zn(O\text{-}2,6\text{-}F_2C_6H_3)_2\cdot THF]_2$, has been shown to be an effective catalyst for the copolymerization of cyclohexene oxide and carbon dioxide to afford high-molecular-weight alternating copolymer, poly(cyclohexenylene carbonate), eq 4. At 80 °C and 55 bar, this catalyst exhibits an average

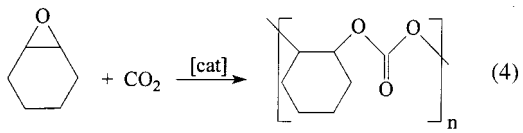

(4)

turnover number of 790 g polym/g Zn for a 48-h reaction period, which translates into a turnover frequency (TOF) of 16.5 g polym/g Zn/hr (see Table 3). Unlike previous zinc phenoxide catalysts and other recently developed catalysts,[4,8] complex **1** is stable in moist air and does not lose activity when it is allowed to stand in a moist oxygen atmosphere for prolonged periods of time. Complex **1** is even more active at catalyzing the homopolymerzation of cyclohexene oxide to provide the polyether, poly(cyclohexenylene oxide), eq 5. This is particularly interesting, because in the copolymerization process, the copolymers that were produced have essentially 100% carbonate

(22) Darensbourg, D. J.; Rainey, P.; Larkins, D. L.; Reibenspies, J. H. *Inorg. Chem.* **2000**, *39*, 473.

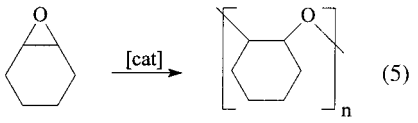

(5)

linkages. The percentage of carbonate linkages is assessed from the integration of the methane protons next to the carbonate linkages ($\delta = 4.60$ ppm) and ether linkages ($\delta = 3.45$ ppm). The copolymers that were produced herein possessed no discernible resonance at 3.45 ppm.

We previously proposed that the lack of successive epoxide ring-opening steps, that is, concurrent polyether formation and polycarbonate production, is the result of the catalyst's possessing only one epoxide binding site. For example, the monomeric bisphenoxide zinc catalysts which contain two labile ether ligands, for example, $Zn(O\text{-}2,6\text{-}t\text{-}Bu_2C_6H_3)_2(THF)_2$, and hence, two epoxide binding sites, generally afford 5−10% ether linkages, even at high CO_2 pressures.[4] However, upon replacing the THF ligands in these derivatives with a single, nonlabile PCy_3 ligand, only one epoxide binding site is present, and as a result, the carbonate linkages in the copolymer are greatly increased without any loss in catalytic activity.[5] Furthermore, this absence of ether linkages in the copolymers when complex **1** is used as catalyst strongly supports the fact that its dimeric structure remains intact during catalysis. This conclusion argues, as well, for the dimeric nature of the PCy_3 zinc derivative, complex **2**, under the conditions of catalytic copolymerization because this derivative was found to be ineffective as a catalyst for the copolymerization of CO_2 and cyclohexene oxide. Recall that $Zn(O\text{-}2,6\text{-}t\text{-}Bu_2C_6H_3)_2{\cdot}PCy_3$ is catalytically active for this process.[5] Similarly, the fully coordinated $Zn(O\text{-}2,6\text{-}F_2C_6H_3)_4^{-2}$ dianion displays no catalytic activity for the coupling of CO_2 and epoxides.

In addition to complex **1**, complexes **6** and **7**, which contain phenoxides with chlorine and bromine substituents, are catalytically active for the production of high-molecular-weight, completely alternating copolymers from CO_2 and cyclohexene oxide. Table 3 lists the turnover numbers and turnover frequencies for the three derivatives for reactions carried out under identical conditions. Similar to complex **1**, complexes **6** and **7** remain active upon exposure to moist air. As seen in Table 3, the catalytic activity for the halogenated phenoxide complexes of zinc decrease as follows: F > Cl > Br. Because at least one of the phenoxides remains in the coordination sphere of the zinc center during chain growth, this trend in reactivity presumably results from an increase in electron density at the zinc center as the electronegativity of the halogen decreases, thereby inhibiting the metal center's binding ability to the epoxide substrate. This, in turn, suggests that epoxide activation is more important than CO_2 insertion in this instance, because the CO_2 insertion process is favored by a more nucleophilic metal-alkoxide moiety.[23,24]

As mentioned earlier, complex **1** is a very efficient catalyst for the polymerization of cyclohexene oxide to polyethers in the absence of CO_2. For example, upon adding the catalyst and cyclohexene oxide to the reactor, polymerization to polyethers takes place prior to the introduction of CO_2; however, once CO_2 is introduced, the copolymerization process dominates. The consequent polymer that was produced is a mixture of poly(cyclohexene oxide carbonate) and poly(cyclohexene oxide ether). Differential scanning calorimetry analysis of the polymer

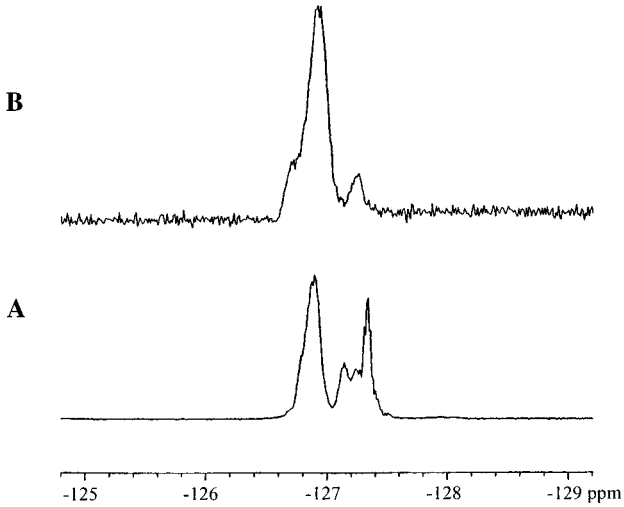

Figure 7. ^{19}F NMR spectra in $CDCl_3$ of polymers produced from reactions catalyzed by $[Zn(O\text{-}2,6\text{-}F_2C_6H_3)_2{\cdot}THF]_2$ (**1**): (a) Low-molecular-weight polycarbonate from cyclohexene oxide and CO_2. (b) Polyether from cyclohexene oxide.

mixture shows two distinct glass transition temperatures at 62.3 °C and 115.2 °C for the polyethers and polycarbonates, respectively. For the terpolymerization of propylene oxide (50 mol %), cyclohexene oxide (50 mol %), and CO_2, the catalyst exhibited an average turnover number of 201 g polym/g Zn and a turnover frequency of 4.19 g polym/g Zn/hr. The formation of cyclic propylene carbonate, which shows an intense asymmetric ν(CO) stretching vibration at 1800 cm^{-1} and is a better ligand for zinc than epoxides, hinders catalytic activity and contributes to the decrease in turnover number and frequency. The polymer that was produced has 84.76 mol % cyclohexene oxide carbonate linkages, 11.90 mol % propylene carbonate linkages, and 3.34 mol % propylene ether linkages. Propylene carbonate and ether linkages show up in the ^1H NMR spectrum at 5.01 and 3.59 ppm, respectively. There are no cyclohexene oxide linkages in the terpolymer. As a result of the incorporation of propylene oxide into the polymer, the T_g is reduced from 115 °C for the cyclohexene oxide copolymer to 101.9 °C for the terpolymer. For the copolymerization of propylene oxide and CO_2, **1** produced only a thin film of polymer. A comparison of cyclic carbonates to polycarbonates produced was determined by infrared spectroscopy, with propylene polycarbonate showing a ν(CO) absorption at 1750 cm^{-1} and cyclic propylene carbonate exhibiting a ν(CO) mode at 1800 cm^{-1}. Under similar reaction conditions to those used in cyclohexene oxide/CO_2 copolymerization, propylene cyclic carbonate is the major product that is produced. However, in agreement with previous work,[4] when the reaction temperature is lowered to 40 °C, propylene polycarbonate is the major product formed. However, this reduction in the amount of cyclic propylene carbonate is not sufficient to stop the poisoning effect of this byproduct to the catalyst.

The presence of the fluorine substituents on complex **1** has allowed us to verify the proposed initiation step in the copolymerization process. Definitive support for initiation involving nucleophile addition of the zinc-bound phenoxide to epoxide or carbon dioxide monomers was obtained by ^{19}F NMR spectroscopy (eq 6). The ^{19}F NMR spectra in $CDCl_3$ of the purified low-molecular-weight copolymer, as well as the polyether, provided by cyclohexene oxide employing complex **1** as catalyst are shown in Figure 7. The spectrum of the copolymer displayed in Figure 7a contains at least four ^{19}F resonances between −126.8 and −127.3 ppm, whereas the corresponding

(23) Darensbourg, D. J.; Sanchez, K. M.; Reibenspies, J. H.; Rheingold, A. L *J. Am. Chem. Soc.* **1989**, *111*, 7094.

(24) Darensbourg, D. J.; Mueller, B. L.; Bischoff, C. J.; Chojnacki, S.; Reibenspies, J. H. *Inorg. Chem.* **1991**, *30*, 2418.

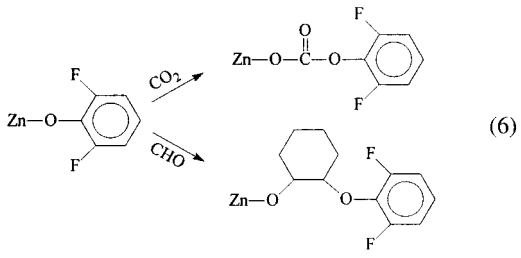

(6)

^{19}F NMR spectrum for the polyether exhibits a broad group of resonances centered at −126.8 ppm. The separation of the two groups of resonances in Figure 7a suggests both CO_2 insertion (−127.3 ppm) and epoxide insertion (−126.8 ppm) as the initial steps in the copolymerization process. This is to be contrasted to the case of sterically encumbering substituents in the 2,6-positions of the bisphenoxide zinc complexes, where initiation by CO_2 insertion at the metal center is prohibited.

Conclusions and Comments

The use of phenolate ligands substituted in the 2,6-positions with sterically unhindered substituents, such as fluorines, has provided dimeric bisphenoxides of zinc and cadmium of the form $[M(O\text{-}2,6\text{-}F_2C_6H_3)_2{\cdot}L]_2$. The metal centers, which are coordinated by two bridging phenoxides and one terminal phenoxide, possess distorted tetrahedral geometries with the fourth ligand(L), THF or PCy_3, accommodated in a trans configuration. ^{31}P NMR spectra of the zinc tricyclohexylphosphine derivative reveal no facile exchange of free and bound phosphine in solution, whereas the cadmium analogue was shown to undergo a rapid equilibration with free PCy_3 in solution via the intermediary of the $Cd(O\text{-}2,6\text{-}F_2C_6H_3)_2(PCy_3)_2$ complex, the latter of which is stabilized relative to the dimer and free PCy_3 at low temperature.

Complex **1**, $[Zn(O\text{-}2,6\text{-}F_2C_6H_3)_2{\cdot}THF]_2$, was shown to be an effective catalyst for the copolymerization of cyclohexene oxide and carbon dioxide and the homopolymerization of cyclohexene oxide. Although the homopolymerization process is the more facile of the two, the copolymerization takes place in a completely alternating manner, that is, with essentially no polyether linkages. This is presumably due to the availability of only one epoxide binding site at the zinc center of complex **1** and supports a dimeric structure for the active catalyst. This latter conclusion is further sustained by the inactivity for catalyzing these polymerization processes of the phosphine adduct of **1**, complex **5**, where the epoxide binding site is occupied by PCy_3. In both polymerization processes, to afford polycarbonates and polyethers utilizing complex **1** as catalyst, the difluorophenoxide end group in the polymers was identified by ^{19}F NMR spectroscopy. The decrease in catalytic activity of the $[Zn(O\text{-}2,6\text{-}X_2C_6H_3)_2{\cdot}THF]_2$ complexes for the copolymerization reaction as the electronegativity of the halogen substituents decreases strongly supports epoxide activation as rate-limiting for chain growth, as opposed to CO_2 insertion. Furthermore, the observation that homopolymerization of cyclohexene oxide to polyethers is much more facile than copolymerization of cyclohexene oxide and CO_2 leads to the conclusion that epoxide ring-opening by a metal-bound alkoxide functionality from the growing polymer chain is much faster than by the corresponding carbonate functionality.

Acknowledgment. Financial support from the National Science Foundation (CHE 99-10342 and CHE 98-07975 for the purchase of X-ray equipment) and the Robert A. Welch Foundation is greatly appreciated. We thank Dr. Robert Taylor for his expertise in obtaining the solid-state and solution ^{113}Cd NMR spectra. We are also grateful to DSM, The Netherlands, for the DSC analysis.

Supporting Information Available: Complete details of the X-ray diffraction study of **1**−**3** and **5**. This material is available free of charge via the Internet at http://pubs.acs.org.

JA002855H